JOURNAL OF APPLIED PHYSICS **109**, 126104 (2011)

Shortening x-ray pulses for pump-probe experiments at synchrotrons

H. A. Navirian,[1] M. Herzog,[1,a)] J. Goldshteyn,[1] W. Leitenberger,[2] I. Vrejoiu,[3] D. Khakhulin,[4]
M. Wulff,[4] R. Shayduk,[1] P. Gaal,[2] and M. Bargheer[1,2]
[1]*Helmholtz-Zentrum Berlin für Materialien und Energie GmbH, Wilhelm-Conrad-Röntgen Campus, BESSY II, Albert-Einstein-Str. 15, 12489 Berlin, Germany*
[2]*Institut für Physik und Astronomie, Universität Potsdam, Karl-Liebknecht-Str. 24-25, 14476 Potsdam, Germany*
[3]*Max-Planck-Institut für Mikrostrukturphysik, Weinberg 2, 06120 Halle, Germany*
[4]*European Synchrotron Radiation Facility (ESRF), 6 rue Jules Horowitz, BP220, 38043 Grenoble, France*

(Received 7 April 2011; accepted 5 May 2011; published online 23 June 2011)

We implemented an experimental scheme for ultrafast x-ray diffraction at storage rings based on a laser-driven Bragg-switch that shortens the x-ray pulses emitted from an undulator. The increased time-resolution is demonstrated by observing changes of intensity, position and width of the diffraction peaks of a $La_{0.7}Sr_{0.3}MnO_3/SrTiO_3$ superlattice sample after optical excitation, i.e., by quantitatively measuring the propagation of an expansion wave through the sample. These experimental transients with timescales of 35 to 60 ps evidence a reduction of the x-ray pulse duration by a factor of two. © *2011 American Institute of Physics*. [doi:10.1063/1.3601057]

Hard x-rays derived from modern synchrotron light sources have ideal properties for structure analysis by x-ray diffraction (XRD). The x-rays are generated by short electron bunches traveling in storage rings, yielding x-ray pulses with a duration on the order of 150 ps. Ultrafast x-ray diffraction (UXRD) uses this time structure in order to access the transient dynamics by pump-probe experiments. An optical pump pulse excites atomic motion in a sample and a time-delayed hard x-ray probe pulse measures the lattice changes for different delay times τ, creating a series of snapshots of the atomic positions. In this stroboscopic scheme the time-resolution is limited by the x-ray pulse duration. One option to obtain ~100 fs x-ray pulses—albeit with relatively low photon flux—is slicing of the electron bunches in an undulator using intense femtosecond laser pulses.[1–3] Because this well-established method is operational at only few beamlines worldwide, and the x-ray free electron lasers (XFELs) will add only few experimental stations,[4] alternative methods are explored. The "low alpha mode" shortens synchrotron pulses considerably, but simultaneously reduces the x-ray flux at all beamlines around the same storage ring.[5,6] Finally, laser-driven x-ray plasma sources have the advantage of being a table-top setup, but lack the tunability of wavelength.[7] The nearly instantaneous drop of the Debye-Waller factor in laser excited InSb was exploited to shorten x-ray pulses, however, this method has not been implemented into a long term stable setup.[8] Recently, we have demonstrated the potential of using coherent phonons in superlattices (SL) to realize switchable Bragg mirrors, which can reduce the pulse duration down to 1 ps (Ref. 9).

In this Communication, we report on the implementation of this scheme at a synchrotron beamline, however, we exploit the somewhat slower change of the Bragg-peak position to truncate the x-ray pulse, instead of the structure-factor change discussed previously which leads to a series of ultrashort x-ray bursts.[9] The modified x-rays diffracted from this Bragg switch (BS), a $SrRuO_3/SrTiO_3$ (SRO/STO) SL, are subsequently used as a probe for the transient x-ray response of a $La_{0.7}Sr_{0.3}MnO_3/SrTiO_3$ (LSMO/STO) SL sample. We demonstrate the shortening of x-ray pulses at the European Synchrotron Radiation Facility (ESRF) by approximately a factor of two down to ~60 ps and we were able to record transients with time scales of 35 ps.

The measurements were performed with 12 keV x-rays from the undulator beamline ID09B at the ESRF, Grenoble, France.[10] The storage ring was operating in the 4-bunch mode with a current of 10 mA per bunch and 708 ns time separation between them. Figure 1 shows a schematic of the setup. A Ti:Sapphire laser providing 600 fs pulses with

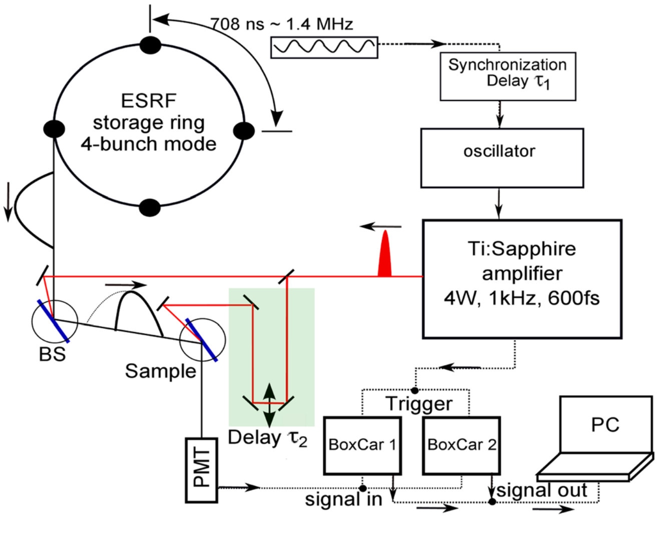

FIG. 1. (Color online) Schematic of the experimental setup. The electronic delay τ_1 gives the relative timing of the first laser pulse and the x-ray pulse at the Bragg switch (BS). The mechanical delay τ_2 sets the timing of the excitation of the sample relative to the x-ray pulse emitted by the BS. Note the schematically illustrated temporal profile of the x-ray pulse before and after diffraction and truncation by the BS.

[a)] Electronic mail: marc.herzog@uni-potsdam.de.

0021-8979/2011/109(12)/126104/3/$30.00

800 nm wavelength at a repetition rate of ~1 kHz was electronically synchronized with the electron-bunch pattern, allowing for a tunable delay τ_1 between laser and x-ray pulses. The timing jitter was on the order of 5 ps, much shorter than the x-ray pulse duration. The laser output was split into two parts, one of which excited the Bragg switch (BS) being the SRO/STO SL described previously with a fluence of 45 mJ/cm^2 (Ref. 9). The second part was guided onto a LSMO/STO SL acting as the sample of interest (fluence of 2.4 mJ/cm^2). This epitaxial heterostructure consists of 15 periods of 13.7 nm thick STO layers and 8.8 nm thick layers of the ferromagnetic metal LSMO grown on a 1 mm STO substrate by pulsed laser deposition[11] as determined from high-resolution XRD. Both the BS and the sample were mounted on independent goniometers enabling individual *xyz*-positioning and adjustment of the Bragg angles (Fig. 1). A mechanical delay line was used to control the relative timing of the pump pulses for the BS and the sample. Since τ_1 was set such that the first laser pulse and the ESRF x-ray pulse were coincident at the BS, the delay line effectively varied the time delay τ_2 between the second laser pulse and the diffracted x-ray pulse at the sample.

The x-ray pulses from the storage ring impinge on the BS at a repetition rate of 1.41 MHz and at a fixed angle Θ_1 defined by the maximum of the (002) zero-order SL peak (ZOP) and are then diffracted toward the sample.[9,12] These pulses are subsequently diffracted from the sample and detected by a plastic scintillator with a rise-time of 1 ns and a Hamamatsu photomultiplier tube (PMT). The analog output of the PMT is electronically gated by two Boxcar integrators which are set to detect x-ray pulses before and after the optical pump pulse, respectively. This way, we are able to evaluate the difference in x-ray intensity diffracted from of the pumped and unpumped sample, respectively, which significantly enhances the signal-to-noise ratio.

In the first part of the experiment, the x-rays diffracted from the BS are directly detected without secondary reflection from the sample. Delay τ_1 was varied to record the transient response of the ZOP peak of the BS [red squares in Fig. 2(a)]. The decreasing signal was fitted using the formula

$$\frac{\Delta R(\tau)}{R_0} = \frac{A}{2}\left\{1 - \operatorname{erf}\left[\frac{4\ln 2(\tau - \tau_0)}{\sigma}\right]\right\} \tag{1}$$

where A, τ_0 and σ are the fitting parameters. Here, σ represents the full width at half-maximum (FWHM) of the Gaussian corresponding to the derivative of Eq. (1) which is also indicated in Figs. 2(b) and (c). The best fit to the data [blue line in Fig. 2(a)] yields $\sigma = 108.5$ ps which is comparable to but slightly smaller than direct streak camera measurements of the ESRF x-ray pulse [$\sigma_{SC} \approx 125$ ps FWHM, dashed line in Fig. 2(a)]. The measured intensity decreases because the Bragg peak position changes to lower angles due to the expansion of the BS triggered by the absorption of the laser pulse.[9,13] The time scale $T^{BS}_{shift} = D_{BS}/v_{eff} \approx 35$ ps for the expansion of the BS is determined by its total thickness ($D_{BS} \approx 250$ nm) and its effective sound velocity, $v_{eff} \approx 7.2$ nm/ps ($v_{SRO} = 6.3$ nm/ps[14] and $v_{STO} = 7.8$ nm/ps[15]) (Refs. 9 and 13). The 108.5 ps time scale measured here is obviously limited by the x-ray pulse duration as it is much longer than the intrinsic dynamics of the Bragg peak. If τ_1 is set to negative values the entire x-ray pulse is reflected from the BS. For large positive τ_1 the Bragg peak position has changed and the diffraction efficiency of the BS at Θ_1 reaches a minimum. At intermediate delays the x-ray pulse is only partly reflected and we expect a truncated x-ray pulse as schematically indicated in Fig. 1.

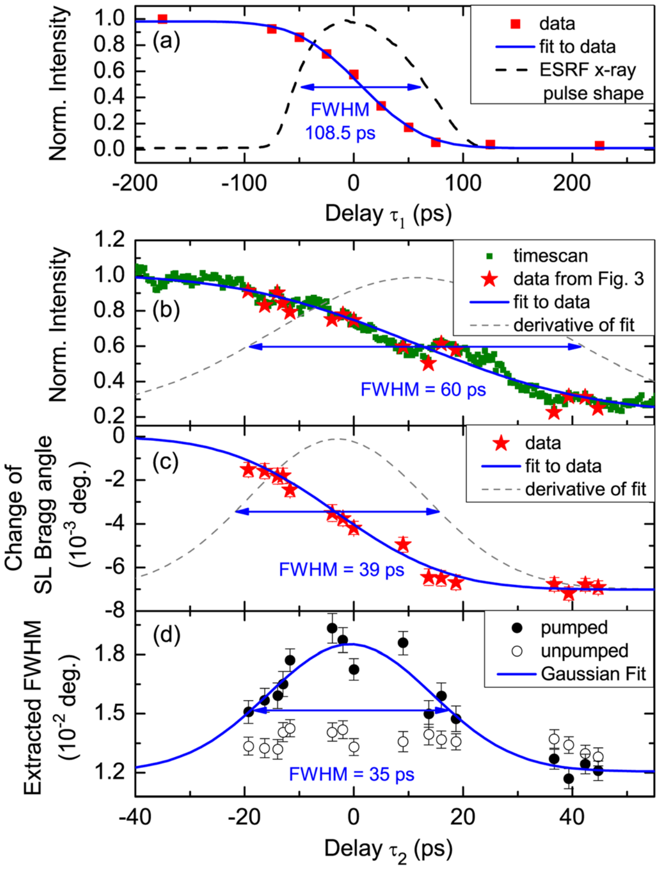

FIG. 2. (Color online) (a) Normalized diffracted intensity of BS vs delay τ_1 (red squares), fit to the data (solid line) and streak-camera characterization of x-ray pulse shape (dashed line). (b) Normalized diffracted intensity of the LSMO/STO ZOP vs delay τ_2 from direct measurement (green squares) and derived from rocking curves in Fig. 3 (red stars), fit to the data (solid line) and scaled derivative of the fit (dashed line). The same delay τ_2 was varied for the next panels: (c) Angular change of the ZOP extracted from Fig. 3 (red stars), fit to the data (solid line) and scaled derivative of the fit (dashed line). (d) Peak width (FWHM) of rocking curves for pumped (bullets) and unpumped sample (circles), and Gaussian fit (solid line).

For the second part of the experiment, we set τ_1 to the value where 60% of the x-ray intensity is reflected and define this as $\tau_1 = 0$ [cf. Figure 2(a)]. At this time delay the laser pulse and the maximum of the x-ray pulse nearly coincide. We aligned the LSMO/STO SL sample to be hit by the diffracted x-ray pulse and scanned the Bragg angle Θ_2 of the sample to obtain the extended rocking curve around the (002) STO substrate reflection shown in the inset of Fig. 3. Fixing Θ_2 at the maximum of the ZOP and scanning τ_2, we recorded the transient presented in Fig. 2(b) which again exhibits a decreasing signal due to the expansion of the LSMO/STO SL. The best fit according to Eq. (1) yields $\sigma = 60$ ps. The sample thickness $D_S \approx 340$ nm and the

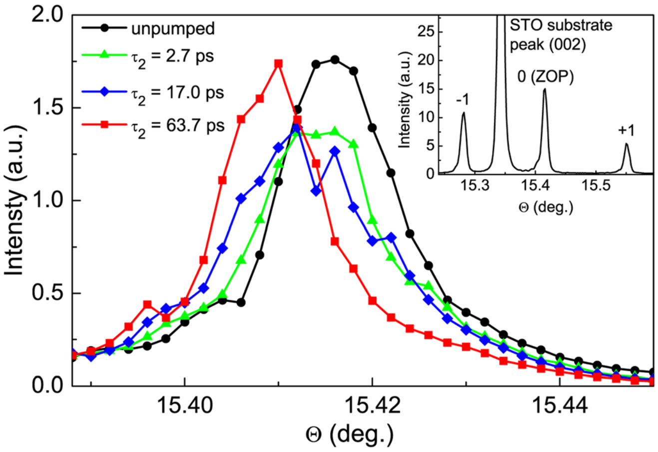

FIG. 3. (Color online) Selected transient rocking curves of the LSMO/STO ZOP used to obtain the data in Figs. 2(b)–(d). Shown are the scaled unpumped (black bullets) and pumped curves at delays $\tau_2 = 2.7$ ps (green triangles), 17.0 ps (blue diamonds) and 63.7 ps (red squares). Inset: Extended static rocking curve around STO substrate peak and ZOP.

sound velocity of LSMO ($v_{\mathrm{LSMO}} = 6.5$ nm/ps[15]) determine the time scale of expansion to be $T^{\mathrm{S}}_{\mathrm{shift}} \approx 47$ ps. Both Figs. 2(a) and (b) measure the intensity decrease caused by the shifting Bragg peaks of the BS and the sample, respectively. The ratios of measured and calculated timescales [108/35 = 3.1 for (a) and 60/47 = 1.3 for (b)] readily suggest that the x-ray pulse probing the sample must have been approximately a factor of two shorter than the 125 ps x-ray pulse of the ESRF, confirming that it was successfully truncated by the BS. We stress that tuning τ_1 to positive (negative) values would truncate the x-ray pulse earlier (later) and would thus diffract shorter (longer) x-ray pulses with an accordingly smaller (larger) total intensity given by Fig. 2(a).

In order to analyze the transient response of the LSMO/STO sample in more detail, several ZOP rocking curves at different pump-probe delays τ_2 were recorded. A selection of these is depicted in Fig. 3. The black curve shows the rocking curve of the unpumped LSMO/STO SL which has to be scaled down to 60% [cf. Figure 2(a)] to give the same integrated intensity as the curves of the pumped sample. The reason is that the x-ray pulses probing the unpumped sample stem from an also unpumped BS so that the full non-truncated x-ray pulse hits the sample. The red curve shows the ZOP at its new position at $\tau_2 = 63.7$ ps, evidencing a relative expansion of $\varepsilon = 0.04\%$. The integrated intensity of the ZOP is constant for all time delays, however, for intermediate times we observe a significant peak broadening as can be directly seen in Fig. 3. In order to quantify the angular change and peak broadening we fitted Gaussian functions to the rocking curves. The extracted peak positions and widths are plotted in Figs. 2(c) and (d), respectively. The data show that the change in peak position (FWHM of ≈39 ps) is accompanied by a transient broadening of the rocking curve (FWHM of ≈35 ps) which is maximal when the peak position is half-way shifted. This behavior is consistent with an expansion wave triggered by the impulsive heating of the LSMO/STO SL. It is launched at the surface of the SL and propagates toward the substrate.[13] When the expansion front has propagated halfway through the SL, one expects a double-peak structure: one peak at the angular position of the unperturbed lattice (black bullets in Fig. 3) and a second peak at the shifted angular position corresponding to the expanded half of the SL (red squares in Fig. 3). Due to the relatively small expansion of 0.04% the separation of these two peaks is rather small and we thus, measure a broadened rocking curve at intermediate times which in principle also includes interference effects.

In conclusion, we have demonstrated a reliable setup for UXRD at synchrotrons where a laser-driven x-ray Bragg switch is used to significantly decrease and control the pulse duration of hard x-rays by truncation of the synchrotron pulses. With these pulses shortened by approximately a factor of two we have performed UXRD experiments on a LSMO/STO SL. Not only an expansion by 0.04% could be detected but, moreover, we could confirm that the laser excitation in such SLs transiently broadens the Bragg reflection because at early times the strain propagation yields different lattice constants at the surface and near the substrate. The same setup is capable of gating the x-ray pulses down to 1 ps using the principle proposed by Herzog *et al.*,[9] however, the excitation laser is required to have a pulse duration ≤ 200 fs in order to efficiently launch the fast SL oscillations.

We thank the BMBF for funding the project via Grant No. 05K10IP1 and the DFG via SFB 762.

[1] R. Schoenlein, S. Chattopadhyay, H. Chong, T. Glover, P. Heimann, C. Shank, A. Zholents, and M. Zolotorev, Science **287**, 2237 (2000).

[2] S. Khan, K. Holldack, T. Kachel, R. Mitzner, and T. Quast, Phys. Rev. Lett. **97**, 074801 (2006).

[3] P. Beaud, S. Johnson, A. Streun, R. Abela, D. Abramsohn, D. Grolimund, F. Krasniqi, T. Schmidt, V. Schlott, and G. Ingold, Phys. Rev. Lett. **99**, 174801 (2007).

[4] B. McNeil, Nat. Photonics **3**, 375 (2009).

[5] M. Abo-Bakr, J. Feikes, K. Holldack, P. Kuske, W. B. Peatman, U. Schade, G. Wüstefeld, and H.-W. Hübers, Phys. Rev. Lett. **90**, 094801 (2003).

[6] I. Radu, C. Stamm, N. Pontius, T. Kachel, P. Ramm, J.-U. Thiele, H. A. Dürr, and C. H. Back, Phys. Rev. B **81**, 104415 (2010).

[7] F. Zamponi, Z. Ansari, C. von Korff Schmising, P. Rothhardt, N. Zhavoronkov, M. Woerner, T. Elsaesser, M. Bargheer, T. Trobitzsch-Ryll, and M. Haschke, Appl. Phys. A **96**, 51 (2009).

[8] J. Larsson, P. Heimann, A. Lindenberg, P. Schuck, P. Bucksbaum, R. Lee, H. Padmore, J. Wark, and R. Falcone, App. Phys. A **66**, 587 (1998).

[9] M. Herzog, W. Leitenberger, R. Shayduk, R. M. van der Veen, C. J. Milne, S. L. Johnson, I. Vrejoiu, M. Alexe, D. Hesse, and M. Bargheer, Appl. Phys. Lett. **96**, 161906 (2010).

[10] M. Wulff, A. Plech, L. Eybert, R. Randler, F. Schotte, and P. Anfinrud, Faraday Discuss. **122**, 13 (2003).

[11] I. Vrejoiu, G. Le Rhun, L. Pintilie, D. Hesse, M. Alexe, and U. Gösele, Adv. Mater. **18**, 1657 (2006).

[12] Here we adopt the notation of SL peak orders described in, e.g., G. Bauer and W. Richter, *Optical Characterization of Epitaxial Semiconductor Layers* (Springer, Berlin, 1996). The SRO/STO (002) ZOP corresponds to the (0 0 116) SL reflection of previous publications.

[13] C. v. Korff Schmising, M. Bargheer, M. Kiel, N. Zhavoronkov, M. Woerner, T. Elsaesser, I. Vrejoiu, D. Hesse, and M. Alexe, Phys. Rev. Lett. **98**, 257601 (2007).

[14] S. Yamanaka, T. Maekawa, H. Muta, T. Matsuda, S. Kobayashi, and K. Kurosaki, J. Solid State Chem. **177**, 3484 (2004).

[15] Y. H. Ren, M. Trigo, R. Merlin, V. Adyam, and Q. Li, Appl. Phys. Lett. **90**, 251918 (2007).